Journal of Cleaner Production 151 (2017) 145–151

Contents lists available at ScienceDirect

Journal of Cleaner Production

journal homepage: www.elsevier.com/locate/jclepro

Effectiveness of municipal sewage sludge (MSS) ash application on the stabilization of Pb-Zn sludge from mining activities

Xingwen Lu [a, b], Kaimin Shih [b], Eddy Y. Zeng [c], Fei Wang [b, c, d, *]

[a] School of Environmental Science and Engineering, Institute of Environmental Health and Pollution Control, Guangdong University of Technology, Guangzhou 510006, China
[b] Department of Civil Engineering, The University of Hong Kong, Pokfulam Road, Hong Kong Special Administrative Region, China
[c] School of Environment, Guangzhou Key Laboratory of Environmental Exposure and Health, and Guangdong Key Laboratory of Environmental Pollution and Health, Jinan University, Guangzhou 510632, China
[d] Guangdong Provincial Key Laboratory of Environmental Pollution Control and Remediation Technology, Guangzhou 510275, China

ARTICLE INFO

Article history:
Received 24 October 2016
Received in revised form
7 February 2017
Accepted 8 March 2017
Available online 8 March 2017

Keywords:
Municipal sewage sludge ash
Pb-Zn sludge
Stabilization
Quantitative X-ray diffraction
Rietveld refinement

ABSTRACT

The feasibility of immobilizing Pb-Zn sludge by sewage sludge ash under thermal conditions was investigated. Sewage sludge ash was found to crystallochemically incorporate Pb into crystalline apatite ($Ca_{5.5}Pb_{4.5}(PO_4)_6(OH)_2$) and stabilize Zn into spinel ($Zn(Al_{0.5}Fe_{1.5})O_4$). The influences of temperature, treatment time and Ca/Pb molar ratio on phase transformation of Pb and Zn were examined to determine the optimal incorporation conditions. The amount of Pb incorporated into $Ca_{5.5}Pb_{4.5}(PO_4)_6(OH)_2$ peaked at 1000 °C, and then decreased with increasing temperature. The immobilization of Zn into $Zn(Al_{0.5}Fe_{1.5})O_4$ was enhanced with increased treatment temperature from 800 °C to 1000 °C and became steady with a further increase of temperature. The most effective treatment time was determined to be 3 h before $Ca_{5.5}Pb_{4.5}(PO_4)_6(OH)_2$ decomposed with prolonged treatment time. The growth of $Ca_{5.5}Pb_{4.5}(PO_4)_6(OH)_2$ and $Zn(Al_{0.5}Fe_{1.5})O_4$ initially increased with an increase in the Ca/Pb molar ratio, reached maximum at a Ca/Pb molar ratio of 9.2/4.5 and dramatically decreased with a further increase of Ca/Pb molar ratio. Prolonged leaching experiments demonstrated the superiority of the sintered mixture of Pb-Zn sludge and MSS ash in stabilizing Zn and Pb. Overall, the present study hinted the feasibility for the beneficial use of sewage sludge ash in immobilizing hazardous Pb-Zn sludge.

1. Introduction

Contamination of soil, groundwater and surface water by hazardous metals is of significant concern due to their toxicity, non-biodegradable properties, accumulative behaviors and diverse sources. Available data from the International Lead and Zinc Study Group estimated that more than 10 million tons of Pb and Zn were consumed globally in 2015, among which 45% of Pb and 43% of Zn were consumed in China. Wastewater generated from the industries engaged in nonferrous smelting, mining and electroplating is the main source of hazardous metals (Liang et al., 2012; Leal Vieira Cubas et al., 2014). Techniques to remove hazardous metals from wastewater and to treat metal-containing effluents often include chemical precipitation, electrochemical treatment, ion exchange, coagulation, adsorption and membrane filtration (Alvarez et al., 2007; Chen et al., 2009a, b; Nanseu-Njiki et al., 2009; Alyüz and Veli, 2009; Athanasiadis and Helmreich, 2005; El Samrani et al., 2008; Guo et al., 2010; Danis and Aydiner, 2009).

However, these treatments often result in large amounts of sludge laden with hazardous metals (Gupta and Subas, 2009). Hazardous metals-containing sludge is often disposed of in controlled landfills, but may contaminate soils, groundwater and surface water due to leaching of hazardous metals (Renou et al., 2008; Zhang et al., 2013; Danthurebandara et al., 2015). In addition, the limited number of landfills has prompted the urgency to develop effective and economical treatment technologies. Pb-Zn sludge was demonstrated to be a suitable aggregate for mortars (Argane et al., 2016) and pigments (Li et al., 2014). To prevent the re-entry of hazardous metals into the environment, hazardous Pb and Zn in sludge should be converted into an insoluble and harmless forms (Scarinci et al., 2000; Rossini and Bernardes, 2006; Li et al., 2007; Zhang, 2013). In this regard, thermal treatment offers

* Corresponding author. Department of Civil Engineering, The University of Hong Kong, Pokfulam Road, Hong Kong Special Administrative Region, China.
E-mail address: wf1984@jnu.edu.cn (F. Wang).

http://dx.doi.org/10.1016/j.jclepro.2017.03.043
0959-6526/

such an advantage, which incorporates hazardous metals into environmental-friendly mineral composites with lower leaching rates than the original materials (Chen et al., 2009a, b; Ndiba et al., 2008; Shih et al., 2006). Previous studies showed that stabilizing hazardous metals (e.g., Pb, Zn, Ni and Cu) into aluminum-rich ceramic matrices can greatly reduce metal leachability via the formation of mineral structures (Shih et al., 2006; Tang et al., 2011a, 2011b; Lu et al., 2013). However, the production of precursor materials (e.g. Al_2O_3, Fe_2O_3, kaolin and mullite) used for the immobilization of these hazardous metals usually requires manufacturing process. Recycling sewage sludge ash as a precursor of materials for the immobilization of hazardous metals in sludge can encourage a more sustainable use of natural resources and also provide economic incentives (Lin et al., 2009).

Wastewater treatment plants continuously produce huge amounts of sewage sludge (Rio et al., 2005), with more than 30 million tons of dry sludge generated annually worldwide (Melero et al., 2015; Krüger and Adam, 2015). Incineration of sewage sludge has been increasingly used in recent years as direct use of sludge in agriculture has caused concerns about food safety (Fullana et al., 2004; Herzel et al., 2015). Incineration can reduce the amount of waste by approximately 70% in mass and 90% in volume; however, residual sewage sludge ash is also produced as another form of waste (Krüger and Adam, 2015). To convert sewage sludge ash into usable products, several recent studies evaluated the feasibility of using sewage sludge ash as a raw material for production of bricks, tiles (Chen and Lin, 2009; Lin et al., 2008; Anderson, 2002), lightweight aggregates (Cheeseman and Virdi, 2005; Chiou et al., 2006), cementitious materials (Li et al., 2012; Husillos-Rodríguez et al., 2013; Lam et al., 2010; Donatello et al., 2010) and ceramics or glass ceramics (Devant et al., 2011; Tian et al., 2011; Donatello and Cheeseman, 2013; Smol et al., 2015).

The major elements in sewage sludge ash are Si, Al, Ca, Fe and P, generally in the crystalline forms of quartz (SiO_2), whitlockites ($Ca_3(PO_4)_2$), hematite (Fe_2O_3) and amorphous phase(s) (Mahieux et al., 2010; Donatello and Cheeseman, 2013; Lynn et al., 2015; Wu et al., 2015), offering the opportunity to create mineral composites for stabilizing hazardous metals. Thus, production of quality ceramics from sewage sludge ash (e.g., outdoor decoration, furnishings, architectural ceramic, sanitary ceramic and etc.) can result in sustainable use of natural resources and also lead to substantial economic incentives. If hazardous metals can be stabilized with the use of sewage sludge ash, a promising waste-to-resource strategy may be developed to reduce environmental hazards and the burden of waste management at the same time. To this end, the present study was conducted to evaluate the feasibility of using sewage sludge ash as an agent for stabilizing hazardous metals in manufacture of ceramic materials. The immobilization efficiency of Pb-Zn sludge with sewage sludge ash was determined to delineate the potential mechanistic processes of Pb-Zn incorporation. The leaching behavior of the sintered samples was then examined to assess the benefits of adopting the waste-to-resource strategy.

2. Materials and methods

2.1. Materials and their characterization

Pb-Zn sludge produced from mining activities was collected from Jiangsu Province of China, homogenously mixed, passed through a 2-mm sieve and dried at 60 °C overnight before being stored in tight plastic containers made of high density polyethylene and polypropylene with the capacity of 1.0 L. Its chemical composition was analyzed with X-ray fluorescence (XRF) (JEOL JSX-3201Z) in three replicates and is displayed in Fig. S1 of the Supplementary data (SD). The contents of crystalline and amorphous phases were identified by quantitative X-ray diffraction (XRD) (SD Fig. S2).

Municipal sewage sludge was collected from the Shatin Sewage Treatment Works in Hong Kong, China, dried at 105 °C for 24 h and heated at 900 °C for 0.5 h, which was used as sludge incineration ash. The treated sludge was ground by ball milling into homogenous fine particles, which were examined by XRD to determine their initial crystal phases (SD Fig. S3) and analyzed by XRF (JEOL JSX-3201Z) to obtain elemental composition (SD Fig. S4).

2.2. Thermal reaction

To examine the transformation patterns of Pb and Zn during thermal treatment, Pb-Zn sludge and sewage sludge ash were mixed with different Ca/Pb ratios, homogenized by ball milling and pressed into pellets with a diameter of 20 mm and a thickness of approximately 5 mm. The pressure to produce pellets was held at 650 MPa for 1 min at room temperature (23 ± 0.5 °C) to ensure consistent compaction of the samples. The pellets were transferred to a muffle furnace and heated at temperatures ranging from 800 to 1100 °C in the air. The dwelling time of sintering ranged from 0.25 to 10 h.

2.3. X-ray diffraction analysis

After thermal treatment, sludge pellets were air-quenched, weighed and ground into powders with particle sizes less than 10 μm for XRD analysis. The X-ray diffraction data were recorded on a Bruker D8 Advance X-ray powder diffractometer equipped with a Cu Kα X-ray tube and a LynxEye detector. The diffractometer was operated at 40 kV and 40 mA, and the 2θ scan ranged from 10° to 80° with a step size of 0.02° and a scan speed of 0.3 s/step. Phase identification was performed with Eva XRD Pattern Processing software (Bruker, Germany) by matching the powder XRD patterns with the standard powder diffraction database published by the International Centre for Diffraction Data. The crystalline phases found in the products include whitlockite [$(CaMg)_3(PO_4)_2$; PDF (Powder Diffraction File) #13-0404], quartz (SiO_2; PDF #86-1630), hematite (Fe_2O_3; PDF #89-0599), palmierite ($K_2Pb(SO_4)_2$; PDF #85-0782), sanidine ($K(Si_3Al)O_8$; PDF #25-0618), Zn aluminium iron spinel ($Zn(Al_{0.5}Fe_{1.5})O_4$; PDF #82-1048), leucite ($KAlSi_2O_6$; PDF #38-1423), hydroxylapatite ($Ca_{10}(PO_4)_6(OH)_2$; PDF #09-432), calcium phosphate ($Ca_3(PO_4)_2$; PDF #09-0169), Pb phosphosulfate ($Pb_4(PO_4)_2SO_4$; PDF #83-0044) and Pb-substituted hydroxyapatite ($Ca_{5.5}Pb_{4.5}(PO_4)_6(OH)_2$; PDF #79-0685).

2.4. SEM-EDS analysis

Fired sludge pellets were polished with submicrometer diamond lapping film and coated with gold for scanning electron microscopic (SEM) characterization (magnification ranging from 20× to 45000×). All SEM analyses were performed on a Hitachi S-4800 SEM system equipped with a secondary electron detector to obtain morphological information and a backscattered electron detector for energy dispersive spectroscopy (EDS).

2.5. Leaching test

The toxicity characteristic leaching procedure (TCLP) designed by the United States Environmental Protection Agency was used to assess the potential hazards of metal-bearing materials (US EPA, 1998; 1992). Acetic acid was used as the leaching fluid to simulate the presence of organic materials in municipal landfill leachate (MacKenzie et al., 2000; Halim et al., 2004). Because short-term TCLP results may lead to misclassification of products (Kosson et al., 2002), extending the duration of the standard leaching

procedure should be more useful for assessing the long-term leaching behavior of metal-bearing materials in the environment. The treated and un-treated sludge samples were tested under a prolonged leaching procedure to evaluate the leachability of hazardous Pb and Zn.

The prolonged leaching procedure was modified from the SW-846 Method TCLP-1311, with a pH 2.9 acetic acid solution (extraction fluid #2) as the leaching fluid. Each leaching vial was filled with 10 mL of TCLP extraction fluid and 0.5 g powders of the treated and un-treated sludge samples. Three duplicates were subject to leaching test. The leaching vials were rotated end-over-end at 60 rpm for 0.75–23 d. At the end of each agitation period, the leachates were passed through 0.2-μm syringe filters and pH was measured. Upon leaching, the concentrations of Pb and Zn in the leachates were determined with an inductively coupled plasma-atomic emission spectrometer (Perkin Elmer Optima 3300DV, Norwalk, CT, USA) with a detection limit less than 0.1 mg L^{-1} (van de Wiel, 2003).

2.6. Rietveld refinement

Rietveld refinements for quantitative analysis of phase composition were processed with the TOPAS (version 4.0) crystallographic program. To monitor the refinement quality, the derived reliability values are provided in SD Tables S1, S2 and S3. A refinement method with CaF_2 as the internal standard (De La Torre et al., 2001; Magallanes-Perdomo et al., 2009; Rendtorff et al., 2010) was used to quantify the amorphous content in samples possibly containing amorphous or poorly crystalline phases. Scans were collected from 10° to 110° 2θ-angle, with a step width of $2\theta = 0.02°$ and a sampling time of 0.5 s per step.

3. Results and discussion

3.1. Effects of temperature on Pb and Zn incorporation efficiency

Fig. 1 shows the XRD patterns for the mixture of Pb-Zn sludge and MSS ash (with a Ca/Pb molar ratio of 5.5/4.5) heated at 800–1100 °C for 3 h. The peak intensity of $Zn(Al_{0.5}Fe_{1.5})O_4$ gradually increased with increasing temperature from 800 °C to 1000 °C, indicative of continuous incorporation of Zn into $Zn(Al_{0.5}Fe_{1.5})O_4$ within the temperature range. For stabilization reactions of Pb, an intermediate Pb-eulytite phase was observed at the temperature range of 800–950 °C. The initial formation of Pb-substituted hydroxyapatite ($Ca_{5.5}Pb_{4.5}(PO_4)_6(OH)_2$) was found at 900 °C. The increase in the peak intensity of $Ca_{5.5}Pb_{4.5}(PO_4)_6(OH)_2$ indicated its crystal growth with increasing temperature from 900 °C to 1000 °C. This was in contrast to a reduction in the amount of the intermediate Pb-eulytite at 800–950 °C, implicating that $Ca_{5.5}Pb_{4.5}(PO_4)_6(OH)_2$ was the more favorable Pb-hosting phase at higher temperatures than Pb-eulytite. The formation of $Ca_{5.5}Pb_{4.5}(PO_4)_6(OH)_2$ highlighted the influence of phosphorous (e.g., biomass) and Ca-containing compounds on the fate of Pb incorporation at high temperatures (900–1000 °C). The peak intensity of the $Ca_{5.5}Pb_{4.5}(PO_4)_6(OH)_2$ phase declined as the temperature increased to 1100 °C. This apparently signaled the beginning of the decomposition of $Ca_{5.5}Pb_{4.5}(PO_4)_6(OH)_2$, which was expected to occur at around 1200 °C (Liao et al., 1999; Bunsiri et al., 2012). It was also reported that the substitution of Ca by Pb in the $Ca_{5.5}Pb_{4.5}(PO_4)_6(OH)_2$ crystal may result in lowered decomposition temperature (Tõnsuaadu et al., 2011).

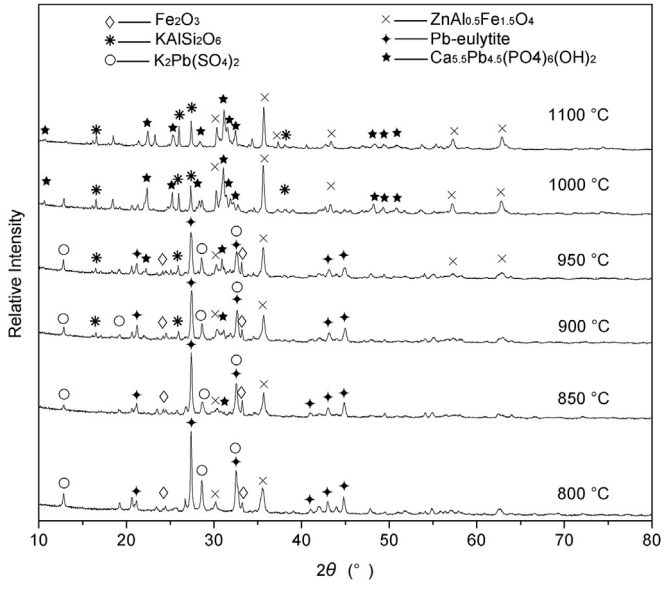

Fig. 1. XRD patterns of sintered lead-zinc sludge and MSS ash with Ca/Pb molar ratio of 5.5/4.5 at temperatures of 800–1100 °C for 3 h.

Apparently Zn and Pb were transformed to $Zn(Al_{0.5}Fe_{1.5})O_4$ and $Ca_{5.5}Pb_{4.5}(PO_4)_6(OH)_2$ by thermally treating Pb-Zn sludge with MSS ash. To quantitatively evaluate the incorporation efficiency of Zn and Pb, the transformation ratios of Zn(TR_{Zn}) and Pb(TR_{Pb}) were determined with quantitative XRD results. TR_{Zn} and TR_{Pb} are defined as follows:

$$TR_{Zn} = [(m_{T'} \times wt_{Zn1} \times (MW_{Zn}/MW_{Zn1}))/(m_T \times wt_{Zn})] \times 100\% \quad (1)$$

$$TR_{Pb} = [(m_{T'} \times wt_{Pb1} \times (MW_{Pb}/MW_{Pb1}))/(mT \times wt_{Pb})] \times 100\% \quad (2)$$

where $m_{T'}$ is the weight of the thermally treated residues; wt_{Zn1} and wt_{Pb1} are the weight per cents of $Zn(Al_{0.5}Fe_{1.5})O_4$ and $Ca_{5.5}Pb_{4.5}(PO_4)_6(OH)_2$, respectively, obtained by quantitative XRD; MW_{Zn}, MW_{Pb}, MW_{Zn1} and MW_{Pb1} are the molecular weights of Zn, Pb, $Zn(Al_{0.5}Fe_{1.5})O_4$ and $Ca_{5.5}Pb_{4.5}(PO_4)_6(OH)_2$, respectively; m_T represents the weight of the Pb-Zn sludge used for the treatment and the values of wt_{Zn} and wt_{Pb} are derived from the XRF results for the initial raw materials.

The compositions of both crystalline and amorphous phases in the products of thermally treated Pb-Zn sludge with MSS ash at 800–1100 °C for 3 h are provided in SD Fig. S5. The TR_{Zn} and TR_{Pb} values were quantified based on the QXRD method by the CaF_2 internal standard. The TR_{Zn} value reached 30% at 800 °C, and the incorporation of Zn into $Zn(Al_{0.5}Fe_{1.5})O_4$ was nearly 100% at 1000 °C (Fig. 2). Increased temperature can facilitate the incorporation of Zn into the $Zn(Al_{0.5}Fe_{1.5})O_4$ in the products. Similarly, TR_{Pb} value increased from 7% to 73% as the temperature was raised from 850 °C to 1000 °C (Fig. 2). The underlying mechanism for the formation of $Zn(Al_{0.5}Fe_{1.5})O_4$ and $Ca_{5.5}Pb_{4.5}(PO_4)_6(OH)_2$ is probably through interfacial reactions between the metals and hosting reactants (hematite, whitlockite and amorphous phase(s)) in MSS ash. The efficiency of interfacial reactions is strongly influenced by the diffusion process between the reactant molecules (Kukukova et al., 2009). Contact of the metals with the hosting reactants from MSS ash was insufficient at 800–900 °C, but was greatly enhanced by higher temperatures (900–1000 °C), resulting in the formation of abundant $Zn(Al_{0.5}Fe_{1.5})O_4$ and $Ca_{5.5}Pb_{4.5}(PO_4)_6(OH)_2$. The TR_{Pb} curve reflected a dramatic decrease in the amount of Pb incorporated into $Ca_{5.5}Pb_{4.5}(PO_4)_6(OH)_2$ at 1100 °C, probably

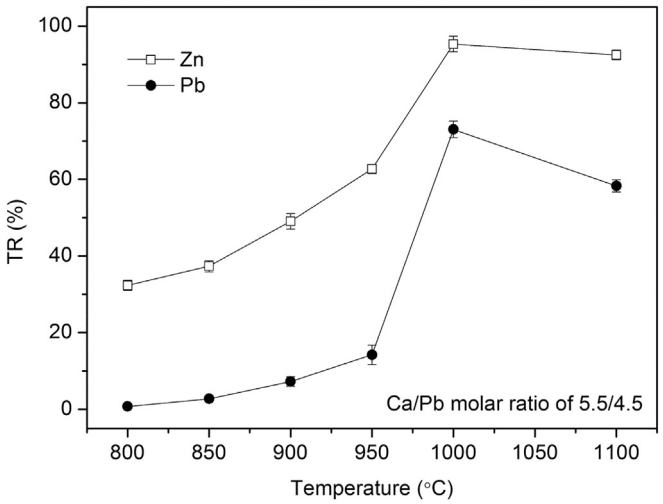

Fig. 2. Effect of temperature on the transformation efficiencies of Zn and Pb by sintering lead-zinc sludge and MSS ash mixtures with Ca/Pb molar ratio of 5.5/4.5 at 800–1100 °C for 3 h.

suggesting thermal decomposition of $Ca_{5.5}Pb_{4.5}(PO_4)_6(OH)_2$ above 1000 °C. To determine the optimal temperature for Pb stabilization, the effect of Pb evaporation was evaluated at 1000–1100 °C. According to the sample weight and XRF data, Pb contents in the 1000 °C and 1100 °C treated products were consistent with their initial compositions, indicating no volatilization of Pb at high temperatures. Thus, 1000 °C can be considered as the most effective temperature for stabilizing Zn and Pb into $Zn(Al_{0.5}Fe_{1.5})O_4$ and $Ca_{5.5}Pb_{4.5}(PO_4)_6(OH)_2$ mineral structures.

3.2. Influence of temperature on product microstructure

The formation of $Zn(Al_{0.5}Fe_{1.5})O_4$ and $Ca_{5.5}Pb_{4.5}(PO_4)_6(OH)_2$ and the textural change of the ceramic matrix under thermal reduction was examined through characterization of the heat-treated products by SEM and EDS. Fig. 3(a) shows the porous product microstructure resulting from the sludge mixture with a Ca/Pb molar ratio of 5.5/4.5 treated at 800 °C for 3 h. The EDS suggested that Pb existed in white-color grains, Fe was enriched in gray regions and the darker-color matrix was enriched by Si (SD Fig. S6). The product grains appeared tightly associated with each other in the sample with a Ca/Pb molar ratio of 5.5/4.5 treated at 1000 °C (Fig. 3(b)). The EDS (SD Fig. S7) presented the chemical compositions of the three distinct areas and the result indicated that the white grains are presumably the $Ca_{5.5}Pb_{4.5}(PO_4)_6(OH)_2$ phase, the gray regions are potentially the $Zn(Al_{0.5}Fe_{1.5})O_4$ phase and the darker matrix is $KAlSi_2O_6$ phase. Together with the XRD results (Fig. 1), the product microstructure and elemental distribution further confirmed the presence of $Ca_{5.5}Pb_{4.5}(PO_4)_6(OH)_2$ (Pb-rich white grains) and $Zn(Al_{0.5}Fe_{1.5})O_4$ (Fe-rich gray regions).

3.3. Effects of time and Ca/Pb ratio on Pb and Zn incorporation efficiency

Rietveld refinement was applied to the XRD patterns of the sintered samples to quantitatively determine the transformation efficiency of Zn and Pb (SD Figs. S8 and S9). The time-dependent transformation ratios of Zn (TR_{Zn}) and Pb (TR_{Pb}) is displayed Fig. 4. Upon sintering for 0.25 h, the TR_{Zn} value reached 20%, and increased to 95% as heating time was extended to 3 h. The transformation of Zn into $Zn(Al_{0.5}Fe_{1.5})O_4$ was close to completion with

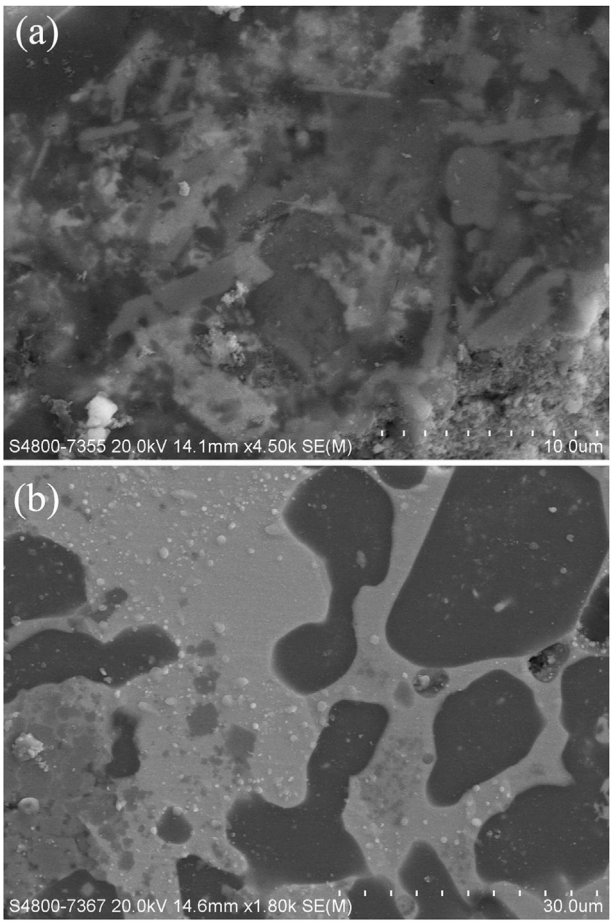

Fig. 3. Scanning secondary electron micrographs of the polished surfaces of the lead-zinc sludge/MSS with Ca/Pb molar ratio of 5.5/4.5 treated at (a) 850 °C and (b) 1000 °C for 3 h.

heating time extended from 3 to 10 h. The TR values of Pb transformation into the $Ca_{5.5}Pb_{4.5}(PO_4)_6(OH)_2$ phase increased gradually from 10% in the first 0.5 h to 72% after 3 h. With treatment time increased to 3 h, $Ca_{5.5}Pb_{4.5}(PO_4)_6(OH)_2$ became the predominant Pb-hosting crystalline phase (SD Fig. S8). The result may suggest

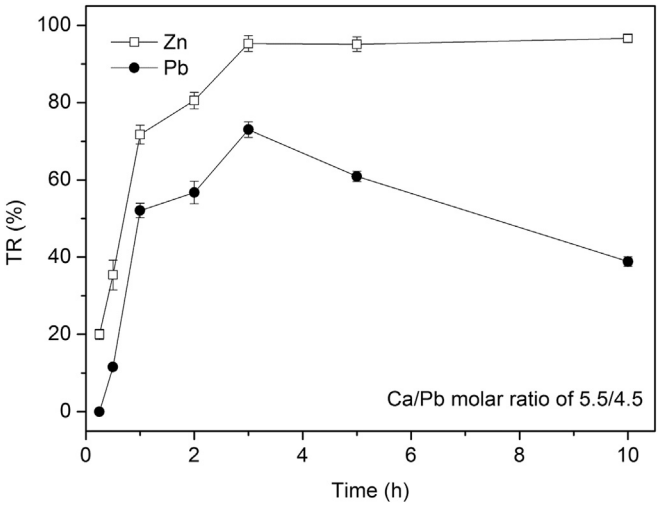

Fig. 4. Values of TR_{Zn} and TR_{Pb} varying with treatment time when lead-zinc sludge and MSS ash with Ca/Pb molar ratio of 5.5/4.5 were sintered at 1000 °C for 0.25–10 h.

that the prolonged sintering time (3 h) enabled a more intensive interaction between Pb and the hosting-reactants, allowing the enhanced molecular transport to overcome the diffusion barrier in the products and promote the formation of $Ca_{5.5}Pb_{4.5}(PO_4)_6(OH)_2$. However, the decomposition of $Ca_{5.5}Pb_{4.5}(PO_4)_6(OH)_2$ led to a decrease of TR_{Pb} with a further increase of treatment time. Therefore, a favorable treatment time of 3 h can be used for the effective incorporation of Pb into $Ca_{5.5}Pb_{4.5}(PO_4)_6(OH)_2$ in the system.

The effects of Ca/Pb molar ratio on the TR_{Zn} and TR_{Pb} were examined by sintering the mixtures of Pb-Zn sludge and MSS ash with different Ca/Pb molar ratios at 1000 °C for 3 h. An increase of Ca/Pb molar ratio from 3.7/4.5 to 9.2/4.5 led to an increase of TR_{Zn} value from 76% to 98% (Fig. 5). However, a dramatic decrease (from 98% to 39%) in Zn incorporation efficacy occurred with increasing Ca/Pb molar ratio from 9.2/4.5 to 22.1/4.5. Similarly, TR_{Pb} was enhanced by decreased Ca/Pb molar ratios (3.7/4.5–9.2/4.5), and reached the maximum efficiency of 87% with a Ca/Pb molar ratio of 9.2/4.5. In addition, a dramatic decrease from 87% to 6% for TR_{Pb} also occurred with an increase of Ca/Pb molar ratio from 9.2/4.5 to 22.1/4.5. Apparently a Ca/Pb molar ratio of 9.2/4.5 was optimal for incorporating the Pb into $Ca_{5.5}Pb_{4.5}(PO_4)_6(OH)_2$ and the Zn into $Zn(Al_{0.5}Fe_{1.5})O_4$. As the efficiency of interfacial reactions is often influenced by the encountering rate between reactant molecules (Klaewkla et al., 2011), sufficient contact of the metals with the hosting-reactants in MSS ash can be achieved with a Ca/Pb molar ratio of 9.2/4.5. The values of TR_{Zn} at 98% and TR_{Pb} at 87% can be achieved with a Ca/Pb molar ratio of 9.2/4.5 at 1000 °C for 3 h.

3.4. Leaching behavior of sintered products

To compare the strategies for stabilizing Zn and Pb under different thermal conditions, the non-heated and two treated samples were selected to determine their differences in Pb and Zn leachability. The pH of each leachate after prolonged leaching is shown in Fig. 6(a). The pH values in the leachates from raw and 800 °C heated sludge mixtures increased in the first 18 h, while those in the leachates from 1000 °C heated mixtures remained similar to initial values throughout the entire leaching period. The increase in leachate pH was likely due to the dissolution of crystal cations through ion exchange with protons in the acidic solution, accompanied by destruction of the crystal structure. Therefore, the small pH change in the leachates from the 1000 °C heated mixtures

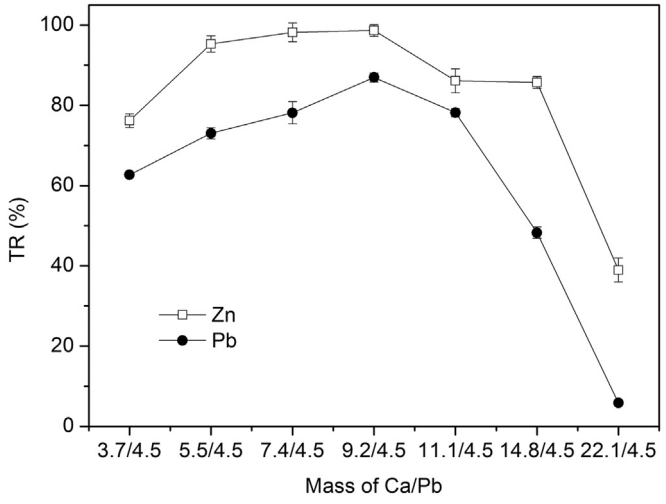

Fig. 5. Effect of Ca/Pb molar ratio on the transformation rates (TR) of Zn and Pb. The TR values were plotted for the 1000 °C and 3 h sintered lead-zinc sludge and MSS ash with different Ca/Pb molar ratios.

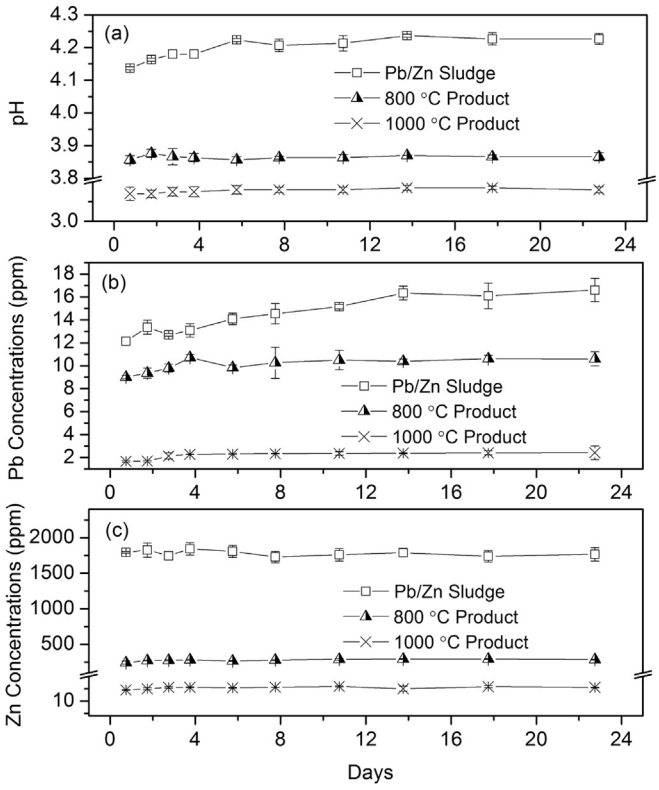

Fig. 6. The temporal variability of (a) pH values; (b) Pb concentrations and (c) Zn concentrations in leachates from lead-zinc sludge/MSS ash before and after sintering at 800 °C and 1000 °C for 3 h.

suggested that they had stronger resistance against acid attack than the raw and 800 °C heated sludge mixtures.

Fig. 6(b) summarizes the concentrations of Pb^{2+} leached from the non-heated, 800 °C and 1000 °C heated samples. The concentration of Pb^{2+} leached from the non-heated sample was nearly 17 ppm, approximately 2 and 7 times greater than those from the 800 °C and 1000 °C heated samples, respectively. Because the Pb-eulytite phase was the major Pb hosting base in the 800 °C heated product, the difference in Pb^{2+} concentrations suggests that the $Ca_{5.5}Pb_{4.5}(PO_4)_6(OH)_2$ crystal structure possesses higher intrinsic resistance to acid attack than the Pb-eulytite phase. The concentrations of Zn^{2+} leached from the non-heated samples were as high as 1800 ppm, more than 6 and 10 times greater than those for the leachates from 800 °C to 1000 °C heated samples, respectively, at the end of the leaching period (Fig. 6(c)). This corroborated the stability of $Zn(Al_{0.5}Fe_{1.5})O_4$ in prolonged leaching and the transformation of Zn to $Zn(Al_{0.5}Fe_{1.5})O_4$ spinel as a highly effective strategy of Zn stabilization.

The current results also showed that leaching of Zn^{2+} and Pb^{2+} from treated samples mostly occurred in the first day. In practical applications, treated samples may be first washed with acid for a short time before they can be safely used as ceramic materials. Therefore, this strategy provides a possible waste-to-resource technique of employing MSS ash for the effective immobilization of hazardous metals in Pb-Zn sludge.

4. Conclusions

The present study explored the potential for immobilization of Zn and Pb in Pb-Ze sludge into $Zn(Al_{0.5}Fe_{1.5})O_4$ and $Ca_{5.5}Pb_{4.5}(PO_4)_6(OH)_2$ structures by thermal treatment with sewage sludge

ash. Overall, 87% of Pb and 98.7% of Zn in sludge were transformed to $Ca_{5.5}Pb_{4.5}(PO_4)_6(OH)_2$ and $Zn(Al_{0.5}Fe_{1.5})O_4$ at 1000 °C after 3 h of sintering. The leachability was lower with 1000 °C heated samples than with untreated samples over a long leaching duration. These results highlighted the feasibility for stabilizing Pb-Zn sludge from mining activities by industrial thermal treatment processes (e.g., incineration and kiln). Furthermore, the utility of sewage sludge ash to incorporate hazardous metals into mineral phases hinted the potential economic use of sludge ash as a ceramic precursor to immobilize hazardous metals under thermal conditions, which is also able to reduce the environmental hazards of Pb-Zn sludge.

Acknowledgments

This research was supported by the National Natural Science Foundation of China (Project No. 41503087), the General Research Fund scheme (HKU 716809E and HKU 716310E) of the Research Grants Council of Hong Kong and the Guangdong Provincial Key Laboratory of Environmental Pollution Control and Remediation Technology (No. 2016K0009).

Appendix A. Supplementary data

Supplementary data related to this article can be found at http://dx.doi.org/10.1016/j.jclepro.2017.03.043.

References

Alvarez, M.T., Crespo, C., Mattiasson, B., 2007. Precipitation of Zn (II), Cu (II) and Pb (II) at bench-scale using biogenic hydrogen sulfide from the utilization of volatile fatty acids. Chemosphere 66 (9), 1677–1683.
Alyüz, B., Veli, S., 2009. Kinetics and equilibrium studies for the removal of nickel and zinc from aqueous solutions by ion exchange resins. J. Hazard. Mater. 167 (1), 482–488.
Anderson, M., 2002. Encouraging prospects for recycling incinerated sewage sludge ash (ISSA) into clay-based building products. J. Chem. Technol. Biot. 77 (3), 352–360.
Argane, R., Benzaazoua, M., Hakkou, R., Bouamrane, A., 2016. A comparative study on the practical use of low sulfide base-metal tailings as aggregates for rendering and masonry mortars. J. Clean. Prod. 112, 914–925.
Athanasiadis, K., Helmreich, B., 2005. Influence of chemical conditioning on the ion exchange capacity and on kinetic of zinc uptake by clinoptilolite. Water Res. 39 (8), 1527–1532.
Bunsiri, R., Thamaphat, K., Limsuwan, P., 2012. Synthesis and characterization of pure natural hydroxyapatite from fish bones bio-waste. Adv. Mater. Res. 506, 206–209.
Cheeseman, C.R., Virdi, G.S., 2005. Properties and microstructure of lightweight aggregate produced from sintered sewage sludge ash. Resour. Conserv. Recyl. 45 (1), 18–30.
Chen, L., Lin, D.F., 2009. Applications of sewage sludge ash and nano-SiO 2 to manufacture tile as construction material. Constr. Build. Mater. 23 (11), 3312–3320.
Chen, Q., Luo, Z., Hills, C., Xue, G., Tyrer, M., 2009a. Precipitation of heavy metals from wastewater using simulated flue gas: sequent additions of fly ash, lime and carbon dioxide. Water Res. 43 (10), 2605–2614.
Chen, Y.L., Shih, P.H., Chiang, L.C., Chang, Y.K., Lu, H.C., Chang, J.E., 2009b. The influence of heavy metals on the polymorphs of dicalcium silicate in the belite-rich clinkers produced from electroplating sludge. J. Hazard. Mater. 170 (1), 443–448.
Chiou, J., Wang, K.S., Chen, C.H., Lin, Y.T., 2006. Lightweight aggregate made from sewage sludge and incinerated ash. Waste Manag. 26 (12), 1453–1461.
Danis, U., Aydiner, C., 2009. Investigation of process performance and fouling mechanisms in micellar-enhanced ultrafiltration of nickel-contaminated waters. J. Hazard. Mater. 162 (2), 577–587.
Danthurebandara, M., Van Passel, S., Vanderreydt, I., Van Acker, K., 2015. Assessment of environmental and economic feasibility of enhanced landfill mining. Waste Manag. 45, 434–447.
De La Torre, A.G., Bruque, S., Aranda, M.A.G., 2001. Rietveld quantitative amorphous content analysis. J. Appl. Crystallogr. 34 (2), 196–202.
Devant, M., Cusidó, J.A., Soriano, C., 2011. Custom formulation of red ceramics with clay, sewage sludge and forest waste. Appl. Clay Sci. 53 (4), 669–675.
Donatello, S., Cheeseman, C.R., 2013. Recycling and recovery routes for incinerated sewage sludge ash (ISSA): a review. Waste Manag. 33 (11), 2328–2340.
Donatello, S., Tyrer, M., Cheeseman, C.R., 2010. Comparison of test methods to assess pozzolanic activity. Cem. Concr. Compos 32 (2), 121–127.
El Samrani, A.G., Lartiges, B.S., Villiéras, F., 2008. Chemical coagulation of combined sewer overflow: heavy metal removal and treatment optimization. Water Res. 42 (4), 951–960.
Fullana, A., Conesa, J.A., Font, R., Sidhu, S., 2004. Formation and destruction of chlorinated pollutants during sewage sludge incineration. Environ. Sci. Technol. 38 (10), 2953–2958.
Guo, M., Qiu, G., Song, W., 2010. Poultry litter-based activated carbon for removing heavy metal ions in water. Waste Manag. 30 (2), 308–315.
Gupta, V.K., Subas, 2009. Application of low-cost adsorbents for dye removal–A review. J. Environ. Manag. 90 (8), 2313–2342.
Halim, C.E., Scott, J.A., Natawardaya, H., Amal, R., Beydoun, D., Low, G., 2004. Comparison between acetic acid and landfill leachates for the leaching of Ph(II), Cd(II), As(V), and Cr(VI) from clementitious wastes. Environ. Sci. Technol. 38 (14), 3977–3983.
Herzel, H., Krüger, O., Hermann, L., Adam, C., 2015. Sewage sludge ash -A promising secondary phosphorus source for fertilizer production. Sci. Total Environ. 542, 1136–1143.
Klaewkla, R., Arend, M., Hoelderich, W.F., 2011. A Review of Mass Transfer Controlling the Reaction Rate in Heterogeneous Catalytic Systems. INTECH Open Access Publisher, Germany.
Kosson, D.S., Van Der Sloot, H.A., Sanchez, F., Garrabrants, A.C., 2002. An integrated framework for evaluating leaching in waste management and utilization of secondary materials. Environ. Eng. Sci. 19 (3), 159–204.
Krüger, O., Adam, C., 2015. Recovery potential of German sewage sludge ash. Waste Manag. 45, 400–406.
Kukukova, A., Aubin, J., Kresta, S.M., 2009. A new definition of mixing and segregation: three dimensions of a key process variable. Chem. Eng. Res. Des. 87, 633–647.
Lam, C.H., Barford, J.P., McKay, G., 2010. Utilization of incineration waste ash residues in Portland cement clinker. Chem. Eng. Trans. 21, 757–762.
Leal Vieira Cubas, A., de Medeiros Machado, M., de Medeiros Machado, M., Gross, F., Magnago, R.F., Moecke, E.H.S., Goncalvez de Souza, I., 2014. Inertization of heavy metals present in galvanic sludge by DC thermal plasma. Environ. Sci. Technol. 48 (5), 2853–2861.
Li, C.T., Lee, W.J., Huang, K.L., Fu, S.F., Lai, Y.C., 2007. Vitrification of chromium electroplating sludge. Environ. Sci. Technol. 41 (8), 2950–2956.
Li, X.G., Lv, Y., Ma, B.G., Chen, Q.B., Yin, X.B., Jian, S.W., 2012. Utilization of municipal solid waste incineration bottom ash in blended cement. J. Clean. Prod. 32, 96–100.
Li, H., Yang, X., Xu, W., Wu, J., Xu, J., Zhang, G., Xia, Y., 2014. Application of dry composite electroplating sludge into preparation of cement-based decorative mortar as green pigment. J. Clean. Prod. 66, 101–106.
Liang, Y.J., Chai, L.Y., Min, X.B., Tang, C.J., Zhang, H.J., Ke, Y., Xie, X.D., 2012. Hydrothermal sulfidation and floatation treatment of heavy-metal-containing sludge for recovery and stabilization. J. Hazard. Mater. 217, 307–314.
Liao, C.J., Lin, F.H., Chen, K.S., Sun, J.S., 1999. Thermal decomposition and reconstitution of hydroxyapatite in air atmosphere. Biomaterials 20 (19), 1807–1813.
Lin, D.F., Chang, W.C., Yuan, C., Luo, H.L., 2008. Production and characterization of glazed tiles containing incinerated sewage sludge. Waste Manag. 28 (3), 502–508.
Lin, K.L., Huang, W.J., Chen, K.C., Chow, J.D., Chen, H.J., 2009. Behaviour of heavy metals immobilized by co-melting treatment of sewage sludge ash and municipal solid waste incinerator fly ash. Waste Manage. Res. 27 (7), 660–667.
Lu, X., Shih, K., Cheng, H., 2013. Lead glass-ceramics produced from the beneficial use of waterworks sludge. Water Res. 47 (3), 1353–1360.
Lynn, C.J., Dhir, R.K., Ghataora, G.S., West, R.P., 2015. Sewage sludge ash characteristics and potential for use in concrete. Constr. Build. Mater. 98, 767–779.
MacKenzie, K.J.D., Temuujin, J., Smith, M.E., Angerer, P., Kameshima, Y., 2000. Effect of mechanochemical activation on the thermal reactions of boehmite (γ-AlOOH) and γ-Al_2O_3. Thermochim. Acta 359 (1), 87–94.
Magallanes-Perdomo, M., Carrodeguas, R.G., Pena, P., De Aza, P.N., De Aza, S., De Aza, A.H., 2009. Non-isothermal devitrification study of wollastonite-tricalcium phosphate bioeutectic® glass. Key Engin. Mater. 396–398, 127–130.
Mahieux, P.Y., Aubert, J.E., Cyr, M., Coutand, M., Husson, B., 2010. Quantitative mineralogical composition of complex mineral wastes–Contribution of the Rietveld method. Waste Manag. 30 (3), 378–388.
Melero, J.A., Sánchez-Vázquez, R., Vasiliadou, I.A., Castillejo, F.M., Bautista, L.F., Iglesias, J., Morales, G., Molina, R., 2015. Municipal sewage sludge to biodiesel by simultaneous extraction and conversion of lipids. Energy Convers. Manag. 103, 111–118.
Nanseu-Njiki, C.P., Tchamango, S.R., Ngom, P.C., Darchen, A., Ngameni, E., 2009. Mercury (II) removal from water by electrocoagulation using aluminium and iron electrodes. J. Hazard. Mater. 168 (2), 1430–1436.
Ndiba, P., Axe, L., Boonfueng, T., 2008. Heavy metal immobilization through phosphate and thermal treatment of dredged sediments. Environ. Sci. Technol. 42 (3), 920–926.
Rendtorff, N.M., Conconi, M.S., Aglietti, E.F., Chain, C.Y., Pasquevich, A.F., Rivas, P.C., Martínez, J.A., Caracoche, M.C., 2010. Phase quantification of mullite-zirconia and zircon commercial powders using PAC and XRD techniques. Hyperfine Interact. 198, 211–218.
Renou, S., Givaudan, J.G., Poulain, S., Dirassouyan, F., Moulin, P., 2008. Landfill leachate treatment: review and opportunity. J. Hazard. Mater. 150 (3), 468–493.
Rio, S., Faur-Brasquet, C., Le Coq, L., Le Cloirec, P., 2005. Structure characterization and adsorption properties of pyrolyzed sewage sludge. Environ. Sci. Technol. 39 (11), 4249–4257.

Rodríguez, N.H., Martínez-Ramírez, S., Blanco-Varela, M.T., Donatello, S., Guillem, M., Puig, J., Fos, C., Larrotcha, E., Flores, J., 2013. The effect of using thermally dried sewage sludge as an alternative fuel on Portland cement clinker production. J. Clean. Prod. 52, 94–102.

Rossini, G., Bernardes, A.M., 2006. Galvanic sludge metals recovery by pyrometallurgical and hydrometallurgical treatment. J. Hazard. Mater. 131 (1), 210–216.

Scarinci, G., Brusatin, G., Barbieri, L., Corradi, A., Lancellotti, I., Colombo, P., Hreglich, S., Dall'Igna, R., 2000. Vitrification of industrial and natural wastes with production of glass fibers. J. Eur. Ceram. Soc. 20, 2485–2490.

Shih, K., White, T., Leckie, J.O., 2006. Spinel formation for stabilizing simulated nickel-laden sludge with aluminum-rich ceramic precursors. Environ. Sci. Technol. 40, 5077–5083.

Smol, M., Kulczycka, J., Henclik, A., Gorazda, K., Wzorek, Z., 2015. The possible use of sewage sludge ash (SSA) in the construction industry as a way towards a circular economy. J. Clean. Prod. 95, 45–54.

Tang, Y., Chui, S.S.Y., Shih, K., Zhang, L., 2011a. Copper stabilization via spinel formation during the sintering of simulated copper-laden sludge with aluminum-rich ceramic precursors. Environ. Sci. Technol. 45 (8), 3598–3604.

Tang, Y., Shih, K., Wang, Y., Chong, T.C., 2011b. Zinc stabilization efficiency of aluminate spinel structure and its leaching behavior. Environ. Sci. Technol. 45 (24), 10544–10550.

Tian, Y., Zuo, W., Chen, D., 2011. Crystallization evolution, microstructure and properties of sewage sludge-based glass–ceramics prepared by microwave heating. J. Hazard. Mater. 196, 370–379.

Tõnsuaadu, K., Gross, K.A., Plūduma, L., Veiderma, M., 2011. A review on the thermal stability of calcium apatites. J. Therm. Anal. Calorim. 110 (2), 647–659.

USEPA, 1992. U.S. EPA Method 1311- Toxicity Characteristic Leaching Procedure and its Salts. Available from: http://www.epa.gov/osw/hazard/testmethods/sw846/pdfs/1311.pdf.

USEPA, 1998. Applicability of the Toxicity Characteristic Leaching Procedure to Mineral Processing Wastes and its Salts. Available from: http://www.epa.gov/osw/nonhaz/industrial/special/mining/minedock/tclp/tcremand.pdf.

van de Wiel, H.J., 2003. Determination of Elements by ICP-AES and ICP-MS. National Institute of Public Health and the Environment (RIVM), Bilthoven, The Netherlands, pp. 1–19.

Wu, D., Tian, Y., Wen, X., Zuo, W., Liu, H., Lee, D.J., 2015. Studies on the use of microwave for enhanced properties of glass-ceramics produced from sewage sludge pyrolysis residues (SSPR). J. Taiwan Inst. Chem. E 48, 81–86.

Zhang, L., 2013. Production of bricks from waste materials–a review. Constr. Build. Mater. 47, 643–655.

Zhang, Q.Q., Tian, B.H., Zhang, X., Ghulam, A., Fang, C.R., He, R., 2013. Investigation on characteristics of leachate and concentrated leachate in three landfill leachate treatment plants. Waste Manag. 33 (11), 2277–2286.